How the Steric Effect Affects Ice Repellency, UV Stability and Corrosion Resistance of Dissimilar *SAMs* Coatings on Al 2024

S. Farhadi[1], M. Farzaneh[1] and S. Simard[2]

[1] Canada Research Chair on Atmospheric Icing Engineering of Power Networks (INGIVRE), Université du Québec à Chicoutimi, QC, Canada

[2]Aluminum Technology Centre, Industrial Materials Institute, National Research Council Canada (CNRC) 501, boul. de l'Université Est, Chicoutimi, QC, Canada

Email: shahram.farhadi@uqac.ca

Abstract: Ice adhesion on outdoor structures is an important issue in cold climate regions. Passive approaches to the problem, e.g. anti-icing or icephobic coatings that inhibit or retard ice accumulation on surfaces, are gaining in popularity. The development of ice-releasing coatings on metallic structures, e.g. Al alloys, is closely related to anti-corrosive protection of that metal, since they must be durable enough when placed in humid environments. In the present study, icephobic stability against UV irradiation and anti-corrosive performance of three dissimilar alkyl-terminated *SAMs* thin films on an aluminium alloy 2024 (AA2024) substrate were investigated. The samples were prepared following wet-chemistry technique by depositing three alkylsilane-based *SAMs* of triethoxy(octyl)silane [$CH_3(CH_2)_7Si(OC_2H_5)_3$, 8C], octadecyltrimethoxysilane [$C_{18}H_{37}Si(OCH_3)_3$, 18C], and trichlorooctadecylsilane [$(CH_3(CH_2)_{17}SiCl_3$, 18C+Cl] on the Al substrate. The influence of the steric effects on coating formation and performance, as well as hydrophobicity and durability versus different pH and/or against UV-irradiation were investigated by means of contact angle measurements, and hydrophobicity losses over time. Glaze ice was artificially deposited on the coated surfaces by spraying supercooled water microdroplets (~65 µm) in a wind tunnel at subzero temperature (-10 °C) to simulate most severe natural atmospheric icing. All samples initially demonstrated ice detachment shear stress values ~ 1.68 to 2 times lower than those of as-received Al surfaces. However, following successive icing/de-icing cycles, different degree of coating degradation was observed. In addition, surface hydrophobicity was studied after icing/de-icing tests to study its stability, showing decreases in contact angle values. Hydrophobicity losses and ice adhesion increase were indeed dramatically and completely different for coated samples with 8C and 18C+Cl *SAMs* compared to 18C *SAMs* thin films. This is probably due to the fact that the 18C *SAMs* was the most ordered thin film among the other two, which is due to the significant influence of the *steric effect*. Meanwhile, potentiodynamic polarization revealed that the corrosion resistance of the coated sample with 18C *SAMs* is slightly improved if compared to the 8C, 18C+Cl and bare samples.

Keywords: steric effects; self-assembling; UV-irradiation; ice adhesion strength; potentiodynamic polarization; coating stability.

INTRODUCTION

Ice and wet snow accumulation hinders the operation and efficiency of infrastructural components, mechanisms and machines, including aircraft, power transmission lines, telecoms equipment, etc. Atmospheric icing occurs when surfaces of exposed structures come into contact with supercooled water droplets or snow particles [1]. Prevention of the icing process requires reducing adhesive strength of ice onto the surface, and therefore, various de-icing and anti-icing techniques have been developed so far, e.g. hydrophobic and superhydrophobic coatings on metallic and non-metallic substrates [2-9]. The ideal solution would be using durable, inexpensive and easy to apply coatings which would reduce ice adhesion to such an extent that ice would fall off under the pull of gravity, e.g. alkyl-terminated coatings [3, 10, 11]. Meanwhile, reasonable correlation between hydrophobicity and ice repellecy was reported earlier [2, 3, 6, 8, 10]. Hydrophobicity can also improve anti-corrosive performance of coated metallic substrates such as Al, as it can prevent penetration of water/aggressive molecules underneath the metallic surface [6-9, 12, 13]. In most studies, ice adhesion on a solid was evaluated by freezing the water artificially on the surface sample under unrealistic icing conditions [14, 15]. Meanwhile, no systematic study on their durability as well as their anti-corrosive performance has been yet reported. Consequently, testing adhesion of glaze ice prepared by spraying supercooled water droplets is expected to give more reliable results [5, 6, 8, 16].

In the present study, icephobicity, stability against UV-irradiation and other aggressive conditions as well as anti-corrosive performance of three dissimilar alkyl-terminated *SAMs* thin films on a aluminium alloy 2024 (AA2024) substrate were investigated. The hydrophobic Al samples were prepared via *"wet-chemistry"* technique, known as an easy-to-apply method, by depositing three alkylsilane-based *SAM*s coatings, as potential ice and snow-repellent layers. The influences of the steric effect on coating performance, their hydrophobicity and durability versus different pH and against UV-irradiation over time were studied by means of contact angle (CA) measurements. Furthermore, a potentiodynamic polarization test was conducted to study corrosion resistance of such prepared coated samples.

I. Experimental procedure

A. *Sample Preparation*

The AA2024-T3 with chemical composition of Al 90.7-94.7wt.%, Si 0.5wt.%, Fe 0.5wt.%, Cu 3.8–4.9wt.%, Mn 0.3-0.9wt.%, Zn 0.25wt.%, Mg 1.2–1.8wt.%, other impurity 0.15wt.% [17] was used as substrate. This alloy is used extensively in applications that require high strength to weight ratio as well as good fatigue resistance. The as-received 2-mm thick Al substrates were ultrasonically cleaned and degreased in water and organic solvents (acetone and ethanol), each for 3 min, followed by cleaning in a *Turco Redoline 53D* alkaline solution (pH~10) for 2-3 min. The alkaline solution was used to create a freshly cleaned Al oxide layer on each surface substrate [18, 19]. The cleaned and polished Al samples were then blow-dried in a N_2 gas flow, and were dried in an oven at 80 °C in air for 3 hrs. They were subsequently placed in corresponding chemical baths of 1% (V/V%) triethoxy(octyl)silane, octadecyltrimethoxysilane, and trichlorooctadecylsilane (from SIGMA-ALDRICH®) at room temperature, abbreviated as 8C, 18C and 18C+Cl *SAMs* coatings (see Fig.1). The solvent was isopropanol, ACS grade, purchased from EMD® .

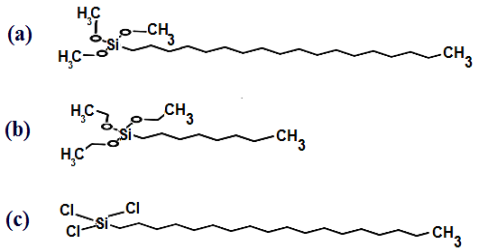

Figure 1: Chemical structure of a) Octadecyltrimethoxysilane (18C), b) Triethoxy(octyl)silane (8C), and c) Trichlorooctadecylsilane (18C+Cl).

Prior to tests or surface characterization, all the coated samples were rinsed ultrasonically with copious amounts of the relevant solvent, isopropanol for 5 sec, followed by blow-drying with N_2. They were finally post-dried in oven at 80 ^oC for 3 hrs and then at 50 ^oC for 5 hrs to remove any volatile components or residual solvents and to improve layer cross-linking [20]. Different concentrations of the silane solutions were tested, but no significant difference was found within a few mM range. The characterization procedures were conducted immediately following sample preparation. While the smaller samples (2 × 2 cm^2) were used to evaluate coatings stability in different conditions, the larger ones (3.2 × 5.2 cm^2) were used to study their ice-repellent performance and corrosion measurements.

B. *Sample charactrization*

Sample stability in water, basic and acidic conditions was studied by means of CA measurements on the samples after immersion in nano-pure water, tap water, as well as in basic (pH: 10.1) and acidic (pH:4) buffer solutions at ~18-20 ^oC. The wetting characteristics, reported in Fig. 2, were obtained following the standard sessile drop method on a DSA100 goniometer from Krüss [4, 6, 16]. For each sample, at least three different spots were randomly measured and the CA reported was the average value of about 5 measurements. Surface topographies were studied by means of scanning electron microscopy (SEM, Hitachi FEGSEM-SU 70) in high-vacuum mode. The X-ray photoelectron spectroscopy (XPS) was performed with a Quantum-2000 instrument from PHI and X-Ray source of achromatic Al Kα. (1486.6 eV). The ice adhesion test was conducted by creating glaze ice (up to ~1 cm thick and ~4-5 gr weight) over a ~3.2 × 3.0 cm^2 surface area and prepared by spraying supercooled micro-droplets of water (average size of ~65 µm) in a wind tunnel at subzero temperature (-10 ^oC), wind speed of 11 ms^{-1}, water pressure of 325 kPa, and water feed rate of 6.3 gm^{-3}. The iced samples were then spun in the centrifuge at constantly increasing speed. Degradation due to UV illumination was assessed using QUV/Accelerated Weathering

Tester in accordance with ASTM G154 and by exposition to a UVA-340 fluorescent lamp to simulate damaging in outdoors conditions in a controlled laboratory environment. Finally, potentiodynamic polarization was used to examine the overall corrosion behaviour of the bare and coated Al samples. The working cell was a standard three-electrode cell with a 1-cm^2 area of the working electrode. A platinized platinum net and saturated calomel electrode (SCE) were used as counter and reference electrode, respectively. The setup used to control the experiments was a potentiostat system composed of a Solartron SI1287A electrochemical interface (controlled by Corrware® software). Measurements were performed in 3.5 wt.% NaCl solutions at room temperature. Potentiodynamic polarization curves were established and the corrosion potential (E_{corr}) and corrosion current density (i_{corr}) were determined using the *Tafel* extrapolation method. The polarization scan was started from 250 mV below the open circuit potential (OCP) in the cathodic region, through the corrosion potential, and 250 mV above the open circuit potential in the anodic region, with a constant scan rate of 1 mVs^{-1}.

II. Results and Discussion

A. Hydrophobicity and Icephobicity of Disimillar SAMs Coatings

Table 1 presents the CA and surface energy values of three dissimilar organosilanes in alkyl chain length and molecular structure on Al substrates. These results were calculated according to Young–Laplace method, as the most theoretically accurate method [16]. It is worthy to mention that prior to use, all baths were vigorously stirred for 3 hrs to allow adequate dissolution/hydrolysis. The hydrolysis/condensation reactions were, indeed, catalyzed by amount of water added to the chemical bath solutions. As it is well known, Al is extremely reactive to atmospheric oxygen, and so has a thin native oxidized surface layer (~4 nm). Thus, it showed water CA and surface energy values of ~41.5±3° (hydrophilic substance) and 46.36±1.64 (mNm^{-1}), respectively. Organosilanes can be easily grafted to a surface by chemical bond (Si-O-Al) demonstrating low surface energy and chemical stability. The XPS signals of C, O and Si, not shown here, showed that the Al surfaces were covered with corresponding *SAMs* coatings. Evidently, by increasing the alkyl chain length, the surface hydrophobicity, CA, was also changed in the following order: 18C+Cl *SAM*s > 18C-*SAM*s > 8C-*SAM*s. The immersion time also plays a significant role in the self-assembly process in terms of surface coverage [21, 22]. Different immersion time periods of 1 min to 120 min were tested. However, the CA corresponding to immersion time of 60 min provided the optimum condition, demonstrating improved wetting properties on the Al substrates.

Table 1: Contact angle and free surface energy [ε (mNm^{-1})] of AA2024 coated with different *SAM*s coatings.

Applied *SAM*s / **Experimental conditions**	**As-received AA2024**	**8C-*SAM*s**	**18C-*SAM*s**	**18C+Cl *SAM*s**
Immersed for 15 min in diluted bath	------	102.2 ± 1° ε: 12.14 (±0.60)	111.4 ± 2° ε: 6.03 (±1.14)	117.1 ± 1° ε: 4.77 (±0.54)
No *SAM*s coating	41.5 ± 3° ε: 46.36 (±1.64)	------	------	------

After coating deposition, all samples demonstrated initial values of contact angle, CA ≥ 100° (Figs.1 and 2), which indicates hydrophobic characteristics. Among these three compounds, the 18C+Cl *SAM*s showed the highest values of CA, which is probably due to erosion of the Al substrate during the *SAM*s process. The CAs of the samples coated with 18C-*SAM*s and 18C+Cl *SAM*s were very close. In contrast, the CA of 8C-coated Al was remarkably smaller than the other two samples. This result suggests that 18C-*SAM*s formed more packed self-assembled thin film on the substrate compared to the 8C-*SAM*s coating. It is also possible that 8C-*SAM*s molecules form film on Al with alkyl chains anchored onto the substrate and that the functional moieties are oriented towards the solution phase, i.e. opposite molecular orientation (formation of -Si-OH bond). This results in more hydrophilicity. Meanwhile, between each layer, the functional trichlorosilane or trimethoxysilane groups can polymerize together through hydrolysis and condensation reaction. This polymer network would provide extra strength to stabilize layer-to-layer interactions. By increasing the alkyl length, the steric effect rises and thus the movement of organosilane moleculs freely decreases. Subsequently, the organosilane hydrolysis/polycondensation becomes more difficult causing the number of organosilane molecules forming a network structure to decrease. Therefore, the network structure becomes thin and the corresponding CAs decreases. When the aliphatic tail is small, the steric effect is dominant. In other words, by increasing the alkyl

chain length, the competition between decrease of reactivity due to the steric effect and the increase of alkyl hydrophobicity caused the difference observed in sample wettability [23]. Now the question is that are these *SAM*s coatings dense enough to prevent aggressive molecules from penetrating through the coatings? Figure 1 shows the CA values of Al samples coated with different silanes as a function of immersion time in nano-pure and tap water as well as basic and acidic media. While these samples initially demonstrated hydrophobicity, however, the CA values decrease over time and lose their hydrophobicity. The coated surfaces were found to gradually lose their hydrophobic properties completely over ~1100-h immersion in different media, associated with a decrease of water CA. This tendency to lose surface hydrophobicity is probably due to a rupture in the Si-O-Al bond between silane molecules and the Al oxide layer due to their hydrolysis. Hydrolysis of Al-O-Si bonds is one of the possible reasons for the silane coatings degradation when they are exposed to aggressive media. This caused hydration of the network and disruption of siloxane and alkyl moieties. The trichlorosilanes contains the corrosive Cl^- ions after hydrolysis. Between the two trimethoxysilane compounds, 18C-*SAM*s has a longer alkyl chain of 18 carbons, while 8C-*SAM*s has a shorter alkyl chain of 8 carbons. This chain length difference may lead to some variations in the structures and properties of the formed thin films. Packing density is expected to increase with chain length [24].

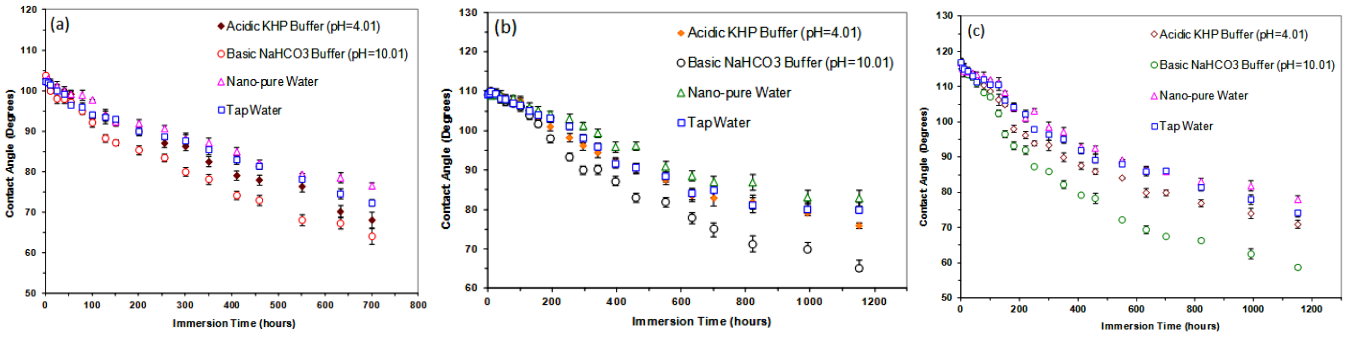

Figure 1: Contact angle of Al sample coated with a) 8C, b) 18C and c) 18C+Cl *SAM*s vs. immersion time in acidic (pH=4.01), basic (pH=10.01), nano-pure and tap water.

It is clear from Figs. 1 and 2 that losing hydrophobicity was faster in the case of samples coated with 8C-*SAM*s and 18C+Cl *SAM*s compared to 18C-*SAM*s. Meanwhile, in all cases, decrease of CA was quiet fast in the case of samples immersed in basic solution in comparison with samples immersed in other media in counterpart. The reason for this observation is attributed to the influence of basic conditions on Al oxide layer stability and the rate of Al corrosion in basic media. Meanwhile, losing hydrophobicity was slightly faster for samples immersed in tap water compared to nano-pure water which is most likely due to influence of salts dissolved in tap water, resulting in accelerated coating deterioration. These *SAM*s layers, indeed, are believed to be not dense enough or too thin with insufficiently cross-linked networks to prevent water molecules/aggressive ions from penetrating through the coating to the surface beneath. In aggressive conditions, the silane layers undergo degradation, and hence, alkylsilane molecules were removed from the surface, resulting in a decrease of surface hydrophobicity.

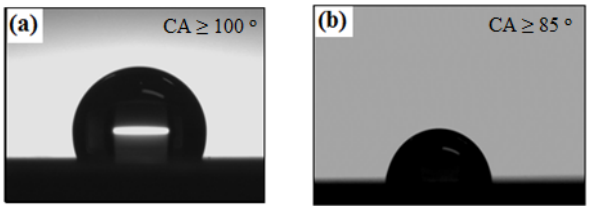

Figure 2: Water droplet on Al surface coated with18C-*SAM*s: a) before and b) after 700-h immersion in nano-pure water.

B) Effect of UV Radiation on Hydrophobic Properties of Prepared SAMs Coatings

Any icephobic coatings must necessarily accomplish both of the following requirements: first, they must efficiently reduce snow/ice adhesion, and second, have a reasonably long service-life (durability). In order to study the durability of coatings in a simulated natural weathering process for potential outdoor applications, their aging performance was studied against UV exposure. The samples were exposed to UVA-340 fluorescent lamp according to ASTM G154. Almost each 537-h of artificial UV exposure is equivalent to one year of sunlight exposure [26]. Figure 3 presents CA values of coated Al samples with different *SAM*s following UV exposure. It is obvious that all samples lost their hydrophobicity associated with a decrease of CA while the number of UV cycles increased. No significant

difference was observed from one sample to another one. Meanwhile, the CA remains almost constant between the 12th to the 20th cycles where the CA slightly decreased. However, after the 20th cycle, the CA reduced dramatically, especially in the case of the sample coated with 8C-*SAM*s where it turns completely hydrophilic. Therefore, based on UV exposure results, it is possible to conclude that a realistic stability was observed for Al coated with 18C-*SAM*s and 18C+Cl *SAM*s over almost six months of natural sunlight exposure. The 8C-*SAM*s exhibits a remarkable UV-induced degradation (reached to ~80^{o} water CA).

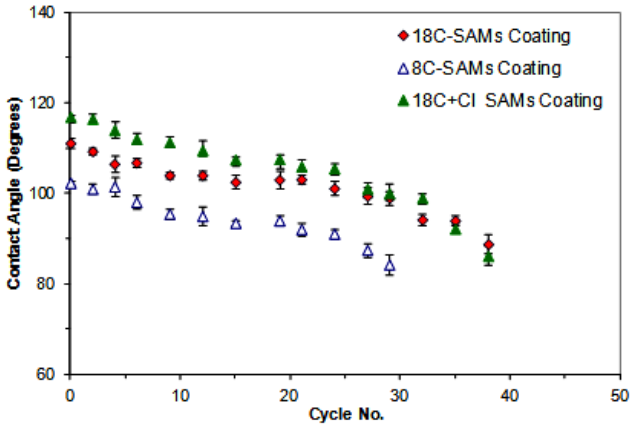

Figure 3: Coating durability (CA vs. UV cycle) for Al coated with different *SAM*s.

C. Ice Adhesion Strength

Each coated Al sample was subjected to 9 successive icing/de-icing cycles. Ice adhesion strength was evaluated as a function of the number of icing/de-icing cycles (Fig.4). While uncoated as-received Al samples showed initial values of ice adhesion strength of ~370±30 kPa, its coated counterparts with 8C-*SAM*s, 18C-*SAM*s and 18C+Cl *SAM*s layers showed reduced values of ~ 220, ~ 190 and ~ 185 kPa, respectively.

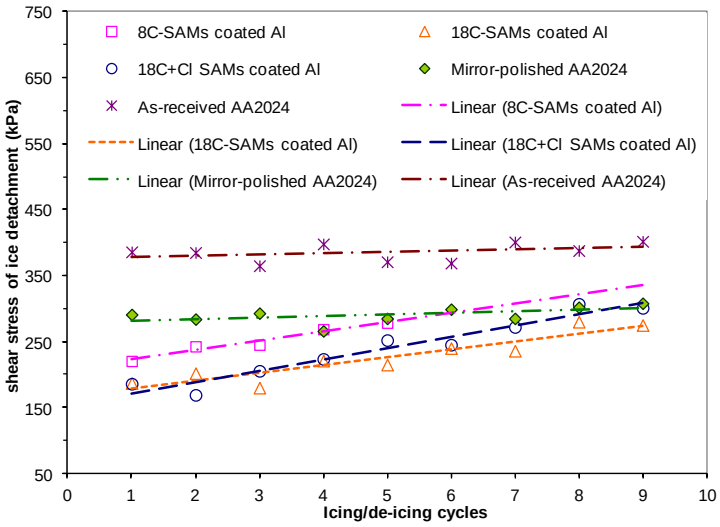

Figure 4: Shear stress of ice detachment *vs.* icing/de-icing for Al surfaces coated with 8C, 18C and 18C+Cl *SAM*s layers.

This reduction can be attributed to the presence of the low surface energy coatings on Al samples. All flat coated surfaces demonstrated shear stress of ice detachment values of ~ 1.68 to 2 times lower than as-received Al surfaces. However, ice adhesion strength increased for both samples, 18C-*SAM*s and 18C+Cl *SAM*s, after as many as 9 icing/de-icing cycles in a similar manner, as shown in Fig.4. This increase in ice adhesion is believed to be associated with partial decay of the coatings caused by their contact with freezing water. The XPS analysis showed that while all coatings demonstrated a peak of Si 2p before test (silane layer(s) on Al), its atomic concentration decreased significantly after ice detachments. Increase in ice adhesion strength was completely different in the case of sample coated with 8C-*SAM*s. It raised the fact that well-ordered 18C-*SAM*s was created on Al surface if compared to *SAM*s of 8C. This decrease was even worse in the case of the sample coated with 8C-*SAM*s. This supports the above mentioned assumption according to

which water molecules hydrolyzed the -O-Si-R bond and gradually destroyed the silane layers on the Al substrate. Meanwhile, the wettability of these samples after several icing/de-icing cycles were studied, showing a gradual decrease in CA values over repeated icing/de-icing cycles.

D. Corrosion resistance of hydrophobic coatings

The potentiodynamic polarization curves of bare and coated AA2024 in 3.5 wt.% NaCl solution are presented in Fig. 5. The $E_{corr.}$, $j_{corr.}$ and R_p values derived from corresponding polarization curves, using Tafel extrapolation, are summarized in Table 2. It is evident in Fig.5 and Table 2 that the value of E_{corr} positively increases from -0.68±0.03V for bare AA2024 to -0.60±0.03V in the case of hydrophobic 18C-*SAM*s coating. However, it shifts slightly to positive values for samples coated with 8C-*SAMs* and 18C+Cl *SAMs*, i.e. -0.64±0.03V and -0.65±0.04V, respectively. This shift obviously corresponds to the improvement in the protective performance of the hydrophobic coating formed on the Al substrate. The 18C-*SAMs* film also showed decrease in $j_{corr.}$ in the cathodic and anodic regions, which suggests a cross-linked network firmly attached to the metallic substrate, leading to protecting the surface against corrosion.

Table 2: Potentiodynamic results of bare and coated AA2024 with 8C-, 18C- and 18C+Cl *SAM*s in 3.5 wt.% NaCl solution.

Specimen	$E_{corr.}$ (V *vs.* SCE)	$j_{corr.}$ (μAcm^{-2})	R_p ($k\Omega cm^2$)
Standard AA2024	-0.68 (±0.03)	22.89 (±.9.06)	2.96 (±2.71)
8C-*SAMs*	-0.64 (±0.03)	4.07 (±1.12)	21.45 (±2.11)
18C+Cl *SAMs*	-0.65 (±0.04)	5.65 (±0.83)	39.24 (±1.21)
18C-*SAMs*	-0.60 (±0.03)	0.90 (±0.11)	248.11 (±2.55)

The slope of anodic current versus E was smaller for 18C-*SAM*s than for the other two coatings that support the fact that this film protects Al surface more effectively.

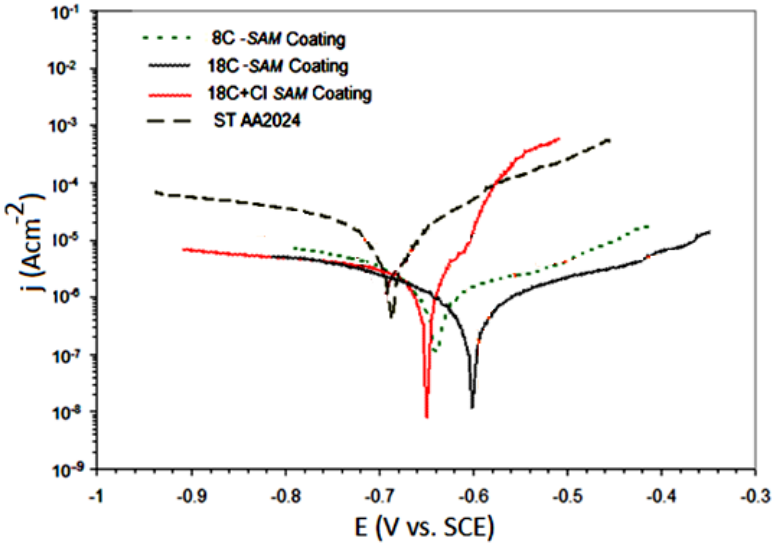

Figure 5: Polarization curves of bare and coated AA2024 with 8C-, 18C- and 18C+Cl *SAMs* coating.

This difference is attributed to the bonding of silane groups to the oxide surface, resulting in enhanced corrosion inhibition. In other words, the corrosion inhibition of 18C-*SAM*s film was superior to those observed for 8C- and 18C+Cl *SAM*s films. It is possible to conclude that according to the polarization results, the 18C-*SAMs* provided a good coverage of the Cu-enriched parts of the AA2024 surface. The Al_2O_3 layer is permeable to electrolytes or moisture and is prone to undergo dissolution in a humid environment, leading to accelerated corrosion. In contrast, the film formed from 18C-*SAMs* is less permeable to corrosion accelerants and thus presents good barrier protection. This is possibly due to presence of less defects in the *SAMs* film of 18C.

IV. Conclusions

In this study, icephobicity, stability in different conditions and against UV-irradiation and anti-corrosive performance of three dissimilar alkyl-terminated *SAMs* thin films on AA2024 were investigated. The hydrophobicity and durability of such coatings in different conditions were tested by means of CA measurements, showing gradual loss of hydrophobicity over time. This was associated with a decrease in CA values of the coated samples. All coated surfaces initially demonstrated shear stress of ice detachment values lower than as-received samples. However, it gradually increased after as many as 5 to 9 successive icing/de-icing cycles due to degradation of coatings upon their contact with freezing water. In addition, the hydrophobic properties of coated surfaces following each ice release presented a slight decrease in CA values. It was showed that hydrophobicity loss and ice adhesion increase were completely different for coated samples with 8C- and 18C+Cl *SAMs* compared to 18C-*SAMs* thin films. It raised the fact that 18C-*SAMs* was more well-ordered than the other *SAMs* mainly due to the significant steric effect on surface properties. Electrochemical measurements showed that the corrosion potential of 18C-*SAMs* increased and its corrosion current density decreased more significantly as compared to that of bare samples. This supports the fact that 18C-*SAMs* demonstrates enhanced corrosion resistance if compared to the 8C- and 18C+Cl *SAMs*.

Acknowledgements

This research work has been conducted within the framework of the NSERC/Hydro-Quebec/UQAC Industrial Chair on Atmospheric Icing of Power Network Equipment (CIGELE) and the Canada Research Chair on Atmospheric Icing Engineering of Power Networks (INGIVRE) at Université du Québec à Chicoutimi. The authors would like to thank the CIGELE partners (Hydro-Québec, Hydro One, Réseau Transport d'Électricité (RTE), Rio Tinto Alcan, General Cable, K-Line Insulators, Dual-ADE, and FUQAC) whose financial support made this research possible.

References

[1] M. Farzaneh, "Atmospheric Icing of Power Networks", Ed., Springer, Berlin, pp. 320, August 2008.
[2] H. Saito, K. Takai, G. Yamauchi, "Water- and ice-repellent coatings". Surface Coatings International, vol. 80, pp. 168–171, 1997.
[3] S. A. Kulinich, M. Farzaneh, "Hydrophobic properties of surfaces coated with fluoroalkylsiloxane and alkylsiloxane monolayers", Surface Science vol. 573, pp. 379–390, 2004.
[4] S. Farhadi, M. Farzaneh, S. Simard, "Nanostructured ultra superhydrophobic Al surfaces: stability and icephobic properties", International Journal of Theoretical and Applied Nanotechnology, vol. 1, pp. 38-44, 2013.
[5] S. A. Kulinich, M. Farzaneh, "How wetting hysteresis influences ice adhesion strength on superhydrophobic surfaces", Langmuir, vol. 25, pp. 8854–8856, 2009.
[6] S. Farhadi, M. Farzaneh, S. A. Kulinich, "Anti-Icing Performance of Superhydrophobic Surfaces", Applied Surface Science, vol. 257, pp. 6264–6269, 2011.
[7] Z. Ghalmi, R. Menini, M. Farzaneh, "Effect of different aluminium surface treatments on ice adhesion strength", Advanced Materials Research, vol. 409, pp. 788-792, 2012.
[8] F. Arianpour, M. Farzaneh, S. Kulinich, "Hydrophobic and ice-retarding properties of doped silicone rubber coatings", Applied Surface Science, vol. 265, pp. 546-552, 2013.
[9] F. Arianpour, M. Farzaneh and S. A. Kulinich, "Nanopowder-Doped Silicone Rubber Coatings for Anti-Ice Applications", Scanning Electron Microscopy, 497 (2010)4.
[10] V. F. Petrenko and S. Peng, "Reduction of ice adhesion to metal by using self-assembling monolayers (*SAMs*)", Can. J. Phys, vol. 8, pp. 387-393, 2003.
[11] M. Farzaneh, "Systems for prediction and monitoring of ice shedding, anti-icing and de-icing for overhead lines", CIGRÉ WG B2.29, CIGRE Publications, Technical Brochure #438, pp. 100, 2010.
[12] Z. Guo, F. Zhou, J. Hao, W. Liu, "Stable Biomimetic super-hydrophobic engineering materials", Journal of the American Chemical Society, vol. 127, pp.15670–15671, 2005.
[13] Y. Shaojun, S. O. Pehkonenb, L. Bin, Y. P. Ting, K.G. Neoh, E. T. Kang, "Superhydrophobic fluoropolymer-modified copper surface via surface graft polymerisation for corrosion protection", Corrosion Science, vol. 53, pp. 2738–2747, 2011.
[14] E. H. Andrews, H. A. Majid, N. A. Lockington, "Adhesion of ice to a flexible substrate", Journal Materials Science, vol. 19, pp. 73-81, 19984.
[15] V. K. Croutch and R. A. Hartley, "Adhesion of ice to coatings and the performance of ice release coatings", *J. Coat. Technol*.**,** vol. 64, pp. 41-52, 1992.
[16] S. Farhadi, M. Farzaneh and S. Simard "On Stability and Ice-Releasing Performance of Nanostructured Fluoro-Alkylsilane-Based Superhydrophobic AA2024 Surfaces", Inter. J. Theor. and Appl. Nanotechnology, 2012.
[17] http://www.matweb.com/search/DataSheet.aspx?MatGUID=57483b4d782940faaf12964a1821fb61.
[18] L. Thomsen, B. Watts, D. Cotton, J. Quinton and P. Dastoor, Surf. Interface Anal., 37 (2005) 472.
[19] X. Yao, Q. W. Chen, L. Xu, Q. K. Li, Y. L. Song, X. F. Gao, D. Quere and L. Jiang, Adv. Funct. Mater., 20 (2010) 656.
[20] S. Farhadi, M. Farzaneh and S. A. kulinich, "Preventing Corrosion and Ice Accretion on Aluminium Surfaces Applying Organic and Inorganic Thin Films", MSc thesis, UQAC, Dec. 2010.
[21] M. J. Pellerite, T. D. Dunbar, L. D. Boardman et al., "Effects of Fluorination on Self-Assembled Monolayer Formation from Alkanephosphonic Acids on Aluminum: Kinetics and Structure", J. Phys. Chem., 107 (2003)11726.
[22] W. Limbut, P. Kanatharana, B. Mattiasson et al., "A comparative study of capacitive immunosensors based on self-assembled monolayers formed from thiourea, thioctic acid, and 3-mercaptopropionic acid" , J. Biosens. Bioelectron., 22 (2006) 233.
[23] M. Jin, S. Li, J. Wanga, et al., Appl. Surf. Sci., 258 (2012) 7552.
[24] M. D. Porter, T. B. Bright, D. L. Allara, C. E. D. Chidsey, J. Am. Chem. Soc. 109 (1987) 3559.
[25] http://www.iso.org/iso/home/store/catalogue_tc/catalogue_detail.htm?csnumber=24372.
[26] ATLAS Weathering Testing Guidebook.